Controlling magnetism with multiferroics

Multiferroics, materials combining multiple order parameters, offer an exciting way of coupling phenomena such as electronic and magnetic order. Using epitaxial growth and heteroepitaxy, researchers have grown high-quality thin films and heterostructures of the multiferroic $BiFeO_3$. The ferroelectric and antiferromagnetic domain structure and coupling between these two order parameters in $BiFeO_3$ is now being studied. We describe the evolution of our understanding of the connection between structure, properties, and new functionalities (including electrical control of magnetism) using $BiFeO_3$ as a model system.

Ying-Hao Chu*, Lane W. Martin, Mikel B. Holcomb, and Ramamoorthy Ramesh

Department of Materials Science & Engineering and Department of Physics, University of California, Berkeley, CA 94720, USA
Materials Sciences Division, Lawrence Berkeley National Laboratory, Berkeley, CA 94720, USA
*E-mail: yhchu@lbl.gov

Magnetoelectric effects in materials provide a great opportunity to use an electric field to control ferromagnetism. Magnetoelectric coupling between electric and magnetic order parameters has been theoretically predicted[1], and there is intense interest in its implementation in device architectures taking advantage of these properties[2–8]. Single-phase multiferroics – materials that show spontaneous magnetization and polarization simultaneously at ambient conditions – remain elusive as most systems (such as the manganites) exhibit mulitferroicity only at low temperatures[9,10]. Alternatively, multiferroics can be synthesized as a composite system, e.g. as a product property of a composite phase consisting of a magnetostrictive and a piezoelectric material[11,12]. Hence, the search continues for new single-phase and composite multiferroic materials that exhibit high ordering temperatures.

One multiferroic material, however, has played a key role in rejuvenating the field after a report of large ferroelectric polarization combined with interesting magnetic properties – $BiFeO_3$ (BFO)[6,13–18]. The large ferroelectric polarization in BFO epitaxial films is in sharp contrast to the weak polarization observed earlier in the bulk[19], but in good agreement with theoretical results[20–23]. Central to the interest in BFO is that it is a room-temperature multiferroic material with both a high ferroelectric Curie temperature[24] and a high antiferromagnetic Néel temperature[25]. Thus it offers exciting potential for room-temperature device integration, if there is coupling between the order parameters[6,20,21,26], as is the case for some multiferroic manganites at low temperatures[5,27,28]. With this in mind, we explore the interplay between structure and properties in the BFO system.

Structure and properties of BFO

The structure of BFO is characterized by two distorted perovskite unit cells (a_r = 3.96 Å, α_r = 0.6°) connected along their body diagonal, denoted by the pseudocubic <111>, to form a rhombohedral unit cell
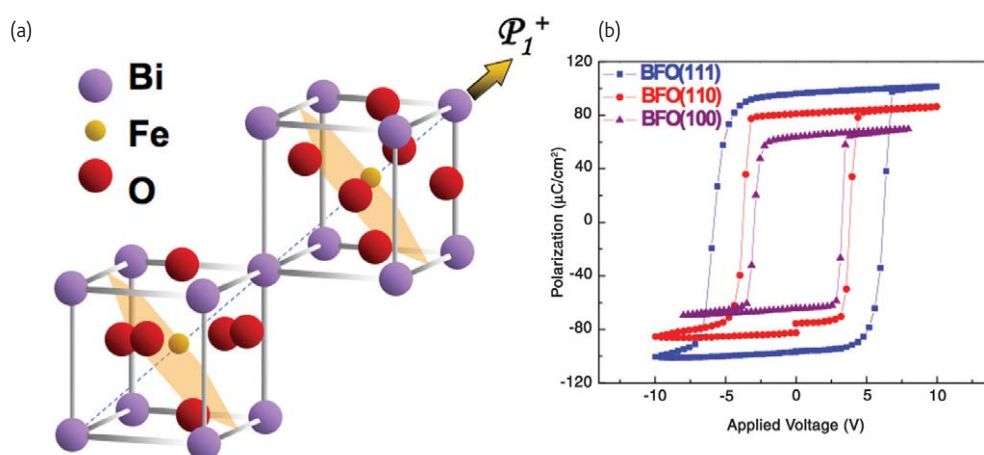
Fig. 1 (a) Schematic of the crystal structure of BFO and the ferroelectric polarization (arrow) and antiferromagnetic plane (shaded planes). (b) Ferroelectric polarization loops measured on epitaxial BFO films with different crystallographic orientations.

(Fig. 1a)[29,30]. The ferroelectric state is realized by a large displacement of the Bi ions relative to the FeO_6 octahedra. This structure results in two important considerations. First, the ferroelectric polarization lies along the pseudocubic <111> leading to the formation of eight possible polarization variants, corresponding to four structural variants[15,30–32]. Second, the antiferromagnetic ordering of BFO is G-type, in which the Fe magnetic moments are aligned ferromagnetically within (111) and antiferromagnetically between adjacent (111). Additionally, BFO is known to exhibit a spin cycloid structure in the bulk[33] and the preferred orientation of the antiferromagnetically aligned spins is in the (111), perpendicular to the ferroelectric polarization direction with six equivalent easy axes within that plane (Fig. 1a)[20]. Antiferromagnetism is therefore coupled to the ferroelectric polarization. Recent studies of BFO thin films have shown the existence of a large ferroelectric polarization, as well as a small net magnetization of the Dzyaloshinskii–Moriya type resulting from a canting of the antiferromagnetic sublattice[20,34].

Studying multiferroic properties in BFO

To explore this material system, it is crucial to study the individual order parameters. This includes investigating both ferroelectric and magnetic properties, as well as the coupling between such order parameters.

In the past, the ferroelectric nature of BFO was unclear, especially since early reports indicated a rather low spontaneous polarization[19]. With the growth of epitaxial thin films of BFO, however, it has become clear that BFO does indeed have a large ferroelectric polarization. At the same time, two limiting factors – trouble with high leakage currents and difficulty in making electrical contacts – remain to be solved. Recent work with BFO films grown on $DyScO_3$ (DSO) substrates has demonstrated the ability to achieve essentially ideal ferroelectric behavior[35]. Sharp ferroelectric loops can be obtained even at low frequencies and measurements indicate low leakage levels.

Furthermore, through studies of substrates with various orientations (Fig. 1b) researchers have been able to demonstrate that the spontaneous polarization in BFO films is indeed along [111] with a magnitude of 90–95 $\mu C/cm^2$, consistent with theoretical calculations.

The ferroelectric domain structure of BFO thin films can be determined and characterized by piezoelectric force microscopy (PFM)[15,16,36]. In this technique, a conductive cantilever with an ac signal induces an alternating electrical field between the tip and the $SrRuO_3$ (SRO) bottom electrode. Local converse piezoelectric vibrations induced by the ac field produce displacements of the film. Using a lock-in technique enables the detection and recording of the sign and phase of the piezoelectric vibration, which can be used in conjunction with crystallographic information to determine the polarization direction in the films. Domains with up- and down-polarizations give rise to opposite contrast in out-of-plane (OP)-PFM images and differences in in-plane components of polarization produce a torque on the atomic force microscope (AFM) cantilever creating contrast in the in-plane (IP)-PFM images. However, domains with polarization vectors along the scanning cantilever's long axis do not give rise to any IP-PFM contrast. On the contrary, domains with polarization pointing to the right with respect to the cantilever's long axis produce an opposite tone to domains with a polarization pointing to the left. This is caused by the antiphase IP-piezoresponse (PR) signals produced by these domains. By combining the OP- and IP-PFM images, therefore, we can identify the polarization direction of each domain. Fig. 2a shows an IP-PFM image of a BFO film grown on a (001) $SrTiO_3$ (STO) substrate. The three contrast levels observed in the IP-PFM images acquired along the two orthogonal <110> directions, together with the uniform OP-PFM contrast (not shown), indicate that the domain structure of the BFO films is characterized by four polarization variants (Fig. 2b). Fig. 2c shows the ferroelectric domain structure for BFO films grown on STO (110) substrates (imaged with the cantilever along [1$\bar{1}$0]). The films exhibit two ferroelectric variants with net polarization pointing 'down'
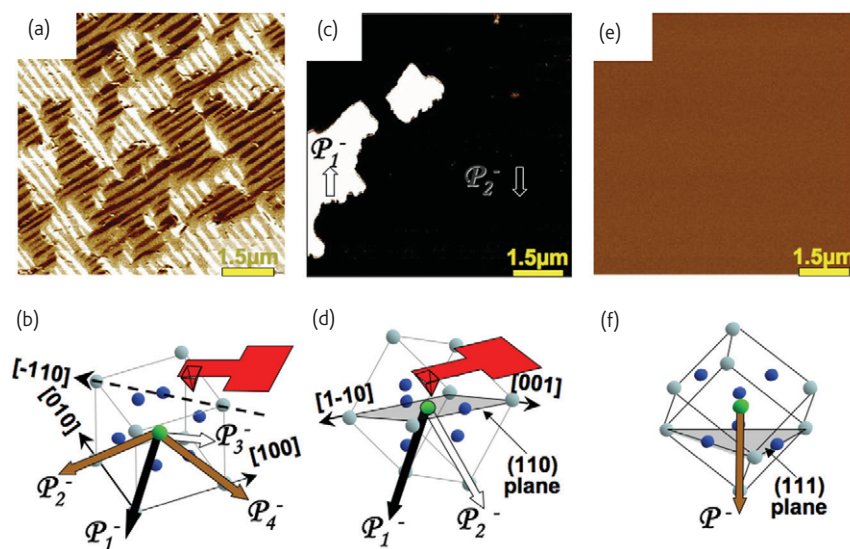
Fig. 2 In-plane PFM images of BFO ferroelectric domain structures on (a) (001), (c) (110), and (e) (111) STO substrates. Schematics of BFO polarization directions and corresponding IP-PFM contrast for (b) BFO (001), (d) (110), and (f) (111).

over large areas (Fig. 2d). BFO films grown on STO (111) substrates exhibit one contrast in the OP-PFM image (not shown) and no contrast in the IP-PFM image (Fig. 2e), suggesting that the polarization direction of the films on STO (111) is perpendicular to the substrate (Fig. 2f). Such domain structures agree well with phase-field models[37] in which the spatial distribution of the polarization field and its evolution is described by time-dependent Ginzburg–Landau equations[38].

Electrical control of multiferroic behavior in BFO films relies on controlling the ferroelectric switching. To switch the films locally, a dc bias is applied to a conducting AFM tip while scanning over the desired area. By analyzing the OP and IP contrast changes following this electrical poling, all three possible switching mechanisms (71°, 109°, and 180°) have been observed (Fig. 3)[16,36]. The red circles indicate the ferroelastic (71° and 109°) switching events, while the remainder of the domains are ferroelectric in nature. In ferroelectric domains with white contrast in OP- and IP-PFM images, 180° switching events are observed as a reversal in both OP- and IP-PFM image contrast (changes to black in both cases). For 71° switching events, only a change in contrast in the OP image is observed (black contrast in OP and white contrast in IP). For 109° switching events, we observe the reverse change in an OP-PFM image (black contrast) but no response from IP-PFM (gray scale).

The antiferromagnetic domain structure of BFO can be studied using photoemission electron microscopy (PEEM) based on X-ray magnetic linear dichroism (XMLD) (Fig. 4)[39–41]. Linear dichroism can arise from any anisotropy in charge distribution in a material. In nonferroelectric antiferromagnets, asymmetry of the electronic charge distribution arising from magnetic order causes a difference in the optical absorption between orthogonal linear polarizations of light[40–43].

This is manifested as a dichroism in the X-ray absorption, which can be used to distinguish different orientations of antiferromagnetic domains. Nonmagnetic ferroelectrics should also show linear dichroism because their polar nature causes an asymmetric electronic charge distribution. Therefore, in BFO, both antiferromagnetic and ferroelectric order should contribute to the dichroism. These two contributions can be separated by the temperature dependence of the XMLD or angle- and polarization-dependent measurements. From this work, it is found that antiferromagnetic and ferroelectric domains are intimately related and match up spatially. The combination of PFM and PEEM, as well as the latter's versatility, is useful for the study of multiferroics.
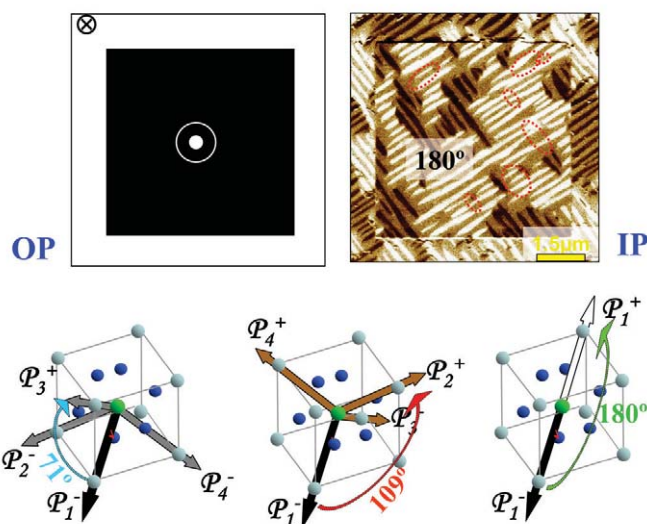

Fig. 3 OP- and IP-PFM images of (001) BFO/SRO/STO films (Fig. 2a) after switching with schematics showing the three possible switching mechanisms.
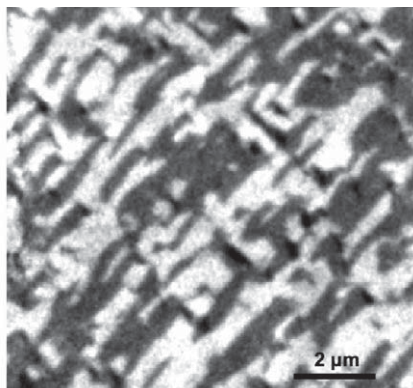
Fig. 4 PEEM allows the study of antiferromagnetism in BFO. Images taken based on XMLD show that the antiferromagnetic domain structure of BFO exactly matches the ferroelectric domain structure.

Magnetoelectric coupling: new functionality

As has been shown, the direction of the polarization can be changed by ferroelectric (180°) and ferroelastic switching events (71° and 109°). At the same time, magnetic moments on the Fe ions couple ferromagnetically within the pseudocubic {111} and antiferromagnetically between adjacent planes[20]. Coupling between the ferroelectric and antiferromagnetic order in BFO is accomplished by the rigid alignment of the antiferromagnetic axis perpendicular to the polarization direction[20]. Thus, certain types of 71° and 109° rotation of the polarization from one <111> axis to one of a specific set of three other <111> axes can result in changes in the magnetic configuration. The ability to control the nature of ferroelectric switching in BFO offers one avenue by which we can study the coupling between ferroelectricity and antiferromagnetism in this material. Through a combination of PFM and PEEM, we have demonstrated coupling between antiferromagnetic and ferroelectric domains during different

Fig. 5 An approach for the electrical control of ferromagnetism. (a) Schematic of our method for electrical control of magnetism. The connection between ferroelectricity (FE), antiferromagnetism (AFM), and ferromagnetism (FM) is shown. (b) Schematic showing the use of BFO films to control the ferromagnetism in CoFe via an exchange-coupling interaction.

ferroelectric switching events[39]. The demonstration of room-temperature magnetoelectric coupling is not only interesting from a fundamental standpoint, but presents great potential for ultimately controlling magnetism with an applied electric field. To use such functionality for device applications, deterministic control not only of antiferromagnetism, but also ferromagnetism, will be essential.

To achieve such a goal, we propose an approach based on the presence of two coupling mechanisms (Fig. 5a). The first is the coupling between ferroelectricity and antiferromagnetism in BFO discussed earlier. Again, it has been shown that we can change the nature of magnetism (antiferromagnetic domain structure) with an applied electric field. The second coupling mechanism of interest is based on a classic exchange coupling interaction[44] that arises at the interface between a ferromagnet and an antiferromagnet (Fig. 5b). Researchers have used such heterostructures to tune the properties of ferromagnets for over 50 years. With the addition of a multiferroic antiferromagnet, however, we now have the potential to control the state of the antiferromagnet electrically and thereby indirectly control the state of the ferromagnet by completing the bottom leg of the coupling triangle in Fig. 5a. Thus the combination of magnetoelectric coupling in a multiferroic and exchange coupling between magnetic materials offers a new pathway for the electrical control of magnetism.

Magnetoelectric coupling: epitaxial strain

Much research has been done on the growth and characterization of epitaxial films because of the significant constraints that heteroepitaxy can impose. Theoretical predictions for heteroepitaxial constrained multiferroic properties can be carried out via first-principles calculations[21,23]. Such treatments suggest that the ferroelectric polarization in multiferroic BFO is almost entirely insensitive to strain. However, the effect of a small monoclinic distortion arising from strain in BFO may lead to a break in the magnetic symmetry and the formation of a preferred antiferromagnetic axis[39]. This added caveat is important because if this were the case, we would expect the antiferromagnetic axis to rotate by 90° only for those ferroelectric switching events that have a 90° rotation of the in-plane component of the polarization. This implies that an added level of control might exist in the realm of magnetoelectric coupling.

In light of these theoretical predictions, a great deal of experimental work has been undertaken to explore the multiferroic nature of epitaxially constrained BFO thin films. High-quality epitaxial BFO films have been prepared by pulsed laser deposition (PLD)[6,45], radio-frequency sputtering[18,46], metal-organic chemical vapor deposition[17,47], and chemical solution deposition on various substrates[48], including STO, DSO, and $LaAlO_3$, with various conducting-oxide electrodes such as SRO, $(La,Sr)MnO_3$, and $LaNiO_3$. The quality of the heterostructures can be demonstrated by using transmission electron microscopy (TEM) (Fig. 6a), with which we can identify the presence of a highly coherent and smooth interface between BFO and the electrode layer.
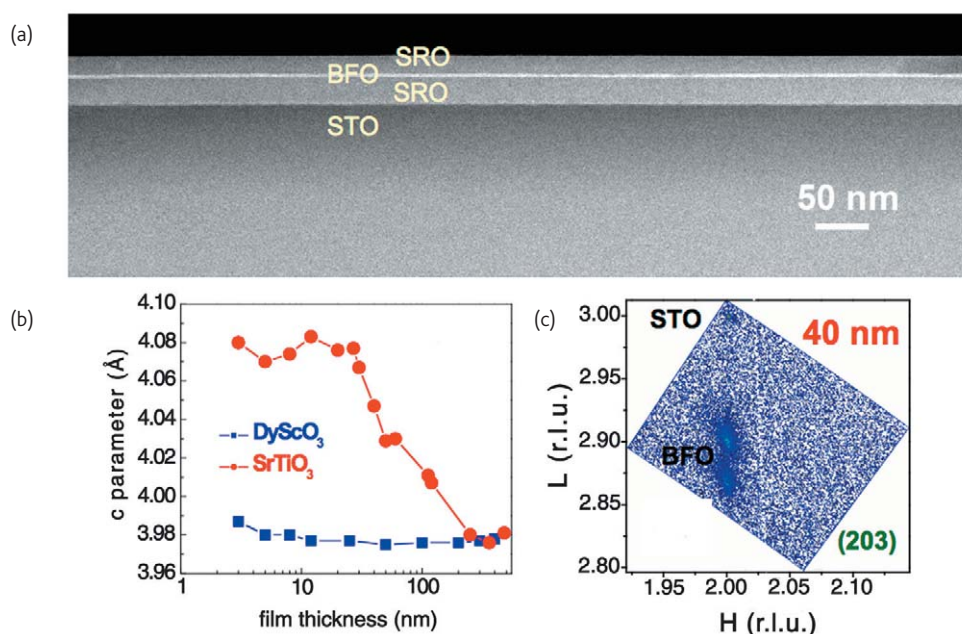
Fig. 6 (a) A typical TEM image of the interfaces between SRO and BFO in a symmetric device structure prepared by the PLD process. The TEM image shows a clear interface between the BFO and SRO layers. (b) Out-of-plane lattice parameter as a function of thickness for BFO films on STO and DSO substrates. (c) A typical reciprocal space map (RSM) represented in reciprocal-lattice units (rlu) for BFO films.

Substrate and film thickness can be varied to study epitaxial strain effects in BFO[49–51]. The out-of-plane lattice parameter is shown in Fig. 6b as a function of BFO film thickness on both STO and DSO substrates. Because of the lattice mismatch between BFO and STO, the BFO lattice is compressed in the in-plane direction and elongated in the out-of-plane direction; this strain gradually decreases with increasing film thickness. For films thinner than ~30 nm, the out-of-plane lattice parameters reach a maximum value implying that a fully epitaxial and maximally strained film has been created. On the contrary, the close lattice match between BFO and DSO means that the out-of-plane lattice parameter remains close to the bulk value.

To understand the effect of strain on the structure of epitaxial BFO films, high-resolution X-ray diffraction (HRXRD) measurements are performed. Reciprocal space mapping (RSM) can also be used to identify the crystal structure of BFO films[52,53]. The BFO lattice is isotropically compressed in the plane of the film because of the lattice mismatch between STO and BFO. Such an effect can lead to the formation of a monoclinically distorted structure for BFO films on STO (001) and (110) substrates. Based on this model, the structural variants of a BFO thin film can also be characterized by detailed RSM measurements[54]. Fig. 6c shows a typical RSM for BFO thin films (<60 nm). The in-plane positions of the 203_{PC} BFO peaks remain almost identical to that of the substrate indicating that the films are fully strained. The splitting between the two peaks reveals the monoclinic angle to be ~0.7° with the distortion direction along [110]. Thicker films (>100 nm) also exhibit peak splitting, indicating a symmetry lower than tetragonal. The in-plane (H-direction) position of the 203_{PC} peaks deviates from the centerline toward smaller values, while the out-of-plane (L-direction) position becomes larger than the thinner films. This suggests that the structure of the film becomes more like the bulk through strain relaxation.

It is apparent that the growth of epitaxially constrained thin films of BFO results in the formation of a slightly distorted structure. But what impact does this, in turn, have on the multiferroic properties? In the monoclinically distorted rhombohedral case, the polarization direction will likely be close to <111>[23]. Based on this, we can interpret the polarization information obtained from PFM measurements. Fig. 7 shows PFM images measured on 9 nm thick BFO samples on DSO
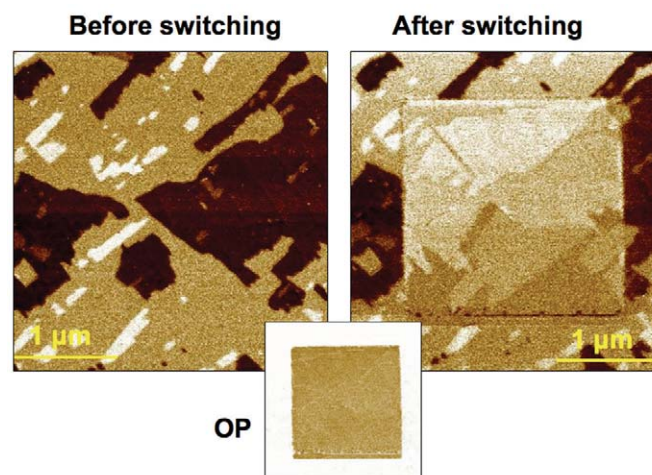

Fig. 7 PFM images of 9 nm (001) BFO/SRO/DSO films (left) before and (right) after switching. This result suggests that the switchable ferroelectric properties remain even for ultrathin BFO films.

substrates before and after switching. Three different contrasts can be found in these images. For all BFO films, the out-of-plane and in-plane PFM images can be explained within the confines of the monoclinically distorted rhombohedral structure with the polarization along <111>. Moreover, using the PFM tip as the top electrode, we can probe the piezoelectric hysteresis of the films locally. All BFO films, down to a thickness of 2 nm, i.e. five BFO unit cells, are switchable[51].

The antiferromagnetic properties of epitaxial BFO have also been studied. Magnetic measurements prove that the cycloidal structure has been broken, which leads to a weak ferromagnetic moment arising from canting of the antiferromagnetic moments in the system[34]. Furthermore, neutron diffraction has been used to obtain insights into the microscopic magnetic structure, confirming the absence of any bulk-like cycloidal modulation in BFO thin films[55]. Finally, using PEEM, a break in the magnetic symmetry, leading to the formation of a preferred antiferromagnetic axis, has been proposed[56], which is consistent with theoretical predictions[39].

Controlling domain structure and switching

At normal operating temperatures for devices, the ferroelectric nature of BFO could dominate the magnetic nature of the system because of the relative robustness of the ferroelectric order parameter. Therefore, controlling the ferroelectric domain structure becomes a critical issue

for device functionality. However, it has also been noted that BFO films can exhibit a very complicated domain structure.

To simplify the domain structure of BFO films, one must induce a break in symmetry for the ferroelectric variants. One way of accomplishing this is through the use of vicinal STO substrates (Fig. 8a)[54]. We have used vicinal substrates miscut along the [010] and [110] directions. The substrates with maximum vicinal angle along [010] correspond to (110) substrates, while those with maximum vicinal angle along [110] correspond to (111) substrates. By using a substrate with a vicinal angle along the [010], the domain structure of BFO films can be limited to exhibit two polarization variants. Stripe patterns, created by two polarization variants 71° apart, with polarization vectors pointing into the substrate, can be observed (Fig. 8b). Similarly, by using a substrate with the miscut along the [110], the formation of one dominant ferroelectric variant can be induced. The same approach can be applied to BFO films grown on STO (110). The two-domain architecture in BFO (110) films can likewise be controlled and evolved into a single domain film on the STO (110) surface. To verify the polarization variants, RSM with line scanning has been used to confirm the domain architecture in these samples (Fig. 8c). This, in conjunction with the fact that epitaxial films on (111) STO with an SRO bottom electrode also exhibit single domain behavior, provides us with a set of model thin-film systems to explore
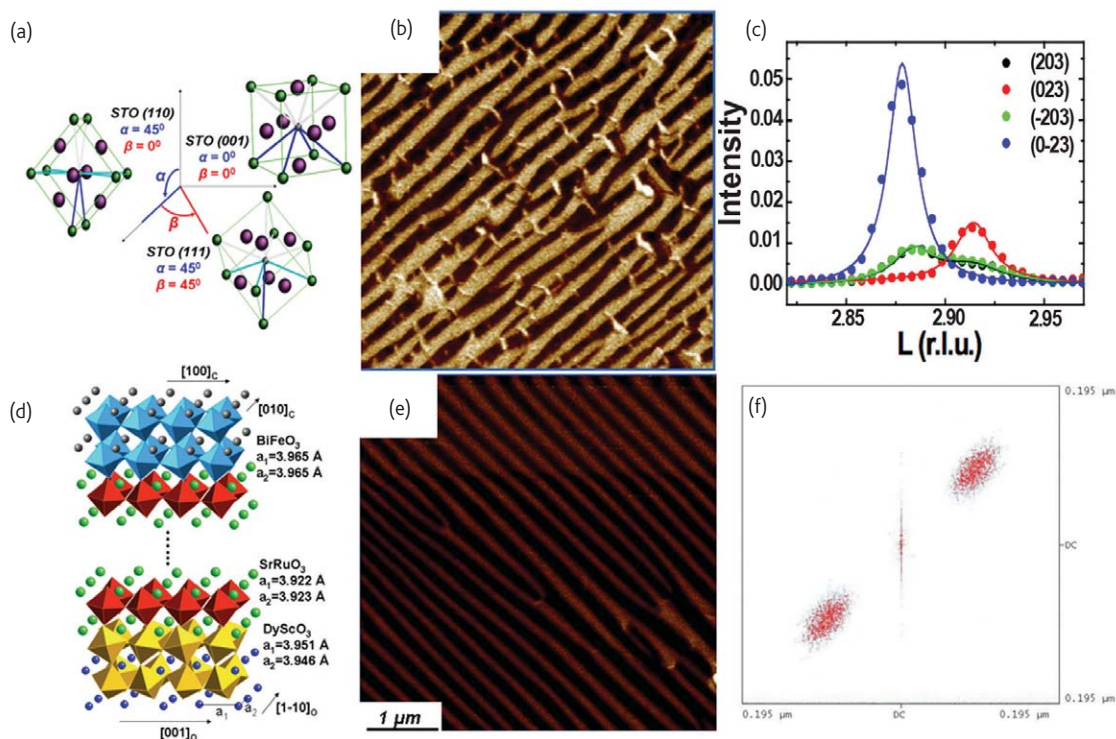

Fig. 8 (a) Schematic of vicinal STO substrates and the corresponding predicted BFO polarization variants on STO(001), (110), and (111) substrates. (b) IP-PFM image of a BFO film on an STO(100) substrate with a 3° miscut along [010]. (c) The {203} line scans of BFO/SRO films grown on STO substrates with two polarization variants. (d) Schematic of the BFO/SRO/DSO heterostructure. (e) IP-PFM images of BFO films with a periodic domain structure. (f) ODP obtained from the periodic PFM image.
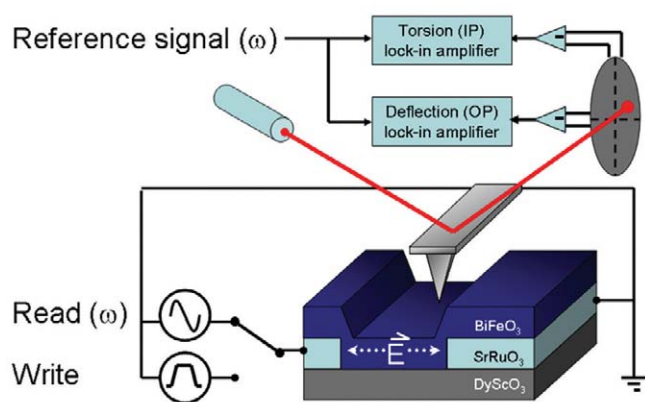
Fig. 9 Schematic of a planar electrode PFM setup. Epitaxial SRO electrodes embedded in the film plane supply an alternating electric field that excites a piezoresponse in the BFO, providing three-dimensional information about the local ferroelectric polarization direction.

the magnetoelectric properties further, as well as the interactions with other layers.

Additionally, multiferroic materials with electrically controllable periodic domain structures (Fig. 8b) could be of great interest for applications in photonic devices. In recent work, an approach to create a one-dimensional periodic domain structure in epitaxial BFO films has been demonstrated[57]. A schematic of the constraints imposed by heteroepitaxy to create long-range order in the domain structure of BFO is shown in Fig. 8d. To achieve this, we first take advantage of the fact that the DSO lattice is very closely matched to that of BFO and SRO. Further, the small structural anisotropy in DSO is used to pin the structure of the SRO layer such that a single domain variant of SRO is formed under the appropriate growth conditions. This structurally simplified SRO film can then used to provide an anisotropic strain that excludes two of the four possible ferroelectric polarization variants and induces a one-dimensional periodic domain structure in BFO films (Fig. 8e). Optical diffraction patterns (ODP) obtained from these PFM images (Fig. 8f), yield an average stripe-domain width of ~200 nm. Having gained control of the underlying domain structure, the next step is to control the nature of the ferroelectric switching events in BFO. The key question in the process is: how can one induce ferroelastic switching and, in turn, stabilize these domains? A combination of phase-field modeling and scanning force microscopy of carefully controlled, epitaxial [110] BFO films with a simplified domain structure reveals that the polarization state can be switched by all three primary switching events through selection of the direction and magnitude of the applied voltage[58]. Moreover, the instability of certain ferroelastic switching processes and domains can be dramatically altered through a judicious selection of neighboring domain walls.

For eventual device applications, the use of a coplanar epitaxial electrode geometry has been proposed to aid in the control of multiferroic switching in BFO (Fig. 9)[59]. PFM has been used to detect and manipulate the striped ferroelectric domain structure of a multiferroic BFO thin film grown on a DSO substrate. Time-resolved

imaging reveals ferroelastic switching of domains in a needlelike region growing from one electrode toward the other. Purely ferroelectric switching is suppressed by the geometry of the electrodes. Such results demonstrate the ability to control the multiferroic order in BFO films by exerting precise control over the ferroelectric order parameter.

The future for multiferroics

The next step in understanding and using the multiferroic order in BFO thin films is to explore the coupling between ferromagnetic layers and BFO. For instance, epitaxial $BFO/La_{2/3}Sr_{1/3}MnO_3$ (LSMO) magnetic tunnel junction heterostructures have been grown[45] without suppressing the ferroelectric order in BFO[49]. Indeed, sizeable tunneling magnetoresistance and exchange-bias effects have been reported on epitaxial BFO/LSMO, BFO/CoFeB[60], and NiFe/BFO[61]. To build on these findings, it is crucial to prove and understand the nature of the coupling mechanism in such heterostructures. We propose the use of PEEM-based measurements as a way to probe this interaction[62]. PEEM, based on XMLD and X-ray magnetic circular dichroism (XMCD), offers high spatial resolution imaging of antiferromagnetic and ferromagnetic domains, respectively. Hence PEEM can be used to elucidate the relationship between the multiferroic BFO and ferromagnetic layers (Fig. 10), which would provide information about how to use an electrical field to control magnetism. Preliminary work in this direction shows considerable promise; and much of our research will remain focused on this exciting possibility. It is also clear that with the current activity and excitement in this field, many new fundamental discoveries are on the horizon that will eventually lead to new applications.

By combining an understanding of the coupling between multiferroic materials like BFO and the ferromagnetic materials listed above, together with our understanding and ability to control the nature of the ferroelectric domains and switching events in BFO,
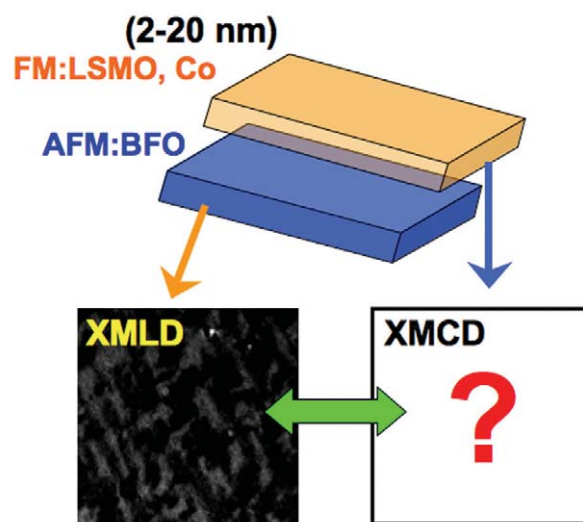

Fig. 10 PEEM offers an avenue to probe and understand the interaction between a multiferroic BFO and a ferromagnetic layer.

we have an unprecedented opportunity to investigate the control of magnetism with an electric field. By using two types of coupling in materials (i.e. magnetoelectric and exchange) (Fig. 5a), we have a route to achieving new functionalities in materials. By controlling the ferroelectric switching in a multiferroic material to maximize the change in the antiferromagnetic structure, we can, in turn, change the nature of the ferromagnetic material coupled to the multiferroic through exchange interactions. The ability to control magnetism with an electric field in this manner, however, remains elusive, but researchers are working hard toward understanding the fundamental materials science and engineering challenges making up this problem.

Conclusions

We have reviewed current research on multiferroic BFO thin films. We have investigated the epitaxial growth of BFO thin films and seen how PFM/PEEM can characterize ferroelectric and antiferromagnetic domain structure and probe the coupling between these two order parameters. We have seen how epitaxial strain, as a function of film thickness, can effect the evolution of ferroelectric and antiferromagnetic order in BFO and how its growth can result in immense changes in the crystalline and domain structure. We have examined how to control domain structure, domain switching mechanisms, and the basic ferroelectric properties of these films. Finally, we have discussed the critical issues that must be solved and the future research directions for this material. Such results are promising for the continued exploration of multiferroic coupling in the magnetoelectric BFO system. BFO provides a model platform to explore the possibility of electrical control of magnetism. mt

Acknowledgments

REFERENCES

1. Landau, L. D., and Liftshitz, E. M., *Electrodynamics of Continuous Media*, Addison-Wesley/Pergamon Press, Oxford, (1960), 119
2. Ramesh, R., and Spaldin, N. A., *Nat. Mater.* (2007) **6**, 21
3. Eerenstein, W., *et al.*, *Nature* (2006) **442**, 759
4. Spaldin, N. A., and Fiebig, M., *Science* (2005) **309**, 391
5. Fiebig, M., *et al.*, *Nature* (2002) **419**, 818
6. Wang, J., *et al.*, *Science* (2003) **299**, 1719
7. Cheong, S. W., and Mostovoy, M. A., *Nat. Mater.* (2007) **6**, 13
8. Prellier, W., *et al.*, *J. Phys. Condens. Matter* (2005) **17**, R803
9. Huang, Z. J., *et al.*, *Phys. Rev. B* (1997) **56**, 2623
10. Hur, N., *et al.*, *Nature* (2004) **429**, 392
11. Srinivasan, G., *et al.*, *Phys. Rev. B* (2002) **65**, 134402
12. Zheng, H., *et al.*, *Science* (2004) **303**, 661
13. Wang, J., *et al.*, *Appl. Phys. Lett.* (2004) **85**, 2574
14. Li, J., *et al.*, *Appl. Phys. Lett.* (2004) **84**, 5261
15. Zavaliche, F., *et al.*, *Appl. Phys. Lett.* (2005) **87**, 182912
16. Zavaliche, F., *et al.*, *Appl. Phys. Lett.* (2005) **87**, 252902
17. Yang, S. Y., *et al.*, *Appl. Phys. Lett.* (2005) **87**, 102903
18. Das, R. R., *et al.*, *Appl. Phys. Lett.* (2006) **88**, 242904
19. Teague, J. R., *et al.*, *Solid State Commun.* (1970) **8**, 1073
20. Ederer, C., and Spaldin, N. A., *Phys. Rev. B* (2005) **71**, 060401(R)
21. Ederer, C., and Spaldin, N. A., *Phys. Rev. B* (2005) **71**, 224103
22. Neaton, J. B., *et al.*, *Phys. Rev. B* (2005) **71**, 014113
23. Ederer, C., and Spaldin, N. A., *Phys. Rev. Lett.* (2005) **95**, 257601
24. Smolenskii, G. A., *et al.*, *Sov. Phys. Solid State* (1961) **2**, 2651
25. Fischer, P., *et al.*, *J. Phys. C: Solid State Phys.* (1980) **13**, 1931
26. Baettig, P., *et al.*, *Phys. Rev. B* (2005) **72**, 214105
27. Kimura, T., *et al.*, *Nature* (2003) **426**, 55
28. Lottermoser, Th., *et al.*, *Nature* (2004) **430**, 541
29. Michel, C., *et al.*, *Solid State Commun.* (1969) **7**, 701
30. Kubel, F., and Schmid, H., *Acta Crystallogr., Sect. B: Struct. Sci.* (1990) **B46**, 698
31. Abplanalp, M., *et al.*, *J. Appl. Phys.* (2002) **91**, 3797
32. Streiffer, S. K., *et al.*, *J. Appl. Phys.* (1998) **83**, 2742
33. Sosnowska, I., *et al.*, *J. Phys. C* (1982) **15**, 4835
34. Bai, F., *et al.*, *Appl. Phys. Lett.* (2005) **86**, 032511
35. Pabst, G. W., *et al.*, *Appl. Phys. Lett.* (2007) **90**, 072902
36. Zavaliche, F., *et al.*, *Phase Transit.* (2006) **79**, 991
37. Zhang, J. X., *et al.*, *J. Appl. Phys.* (2007) **101**, 114105
38. Chen, L. Q., *Annu. Rev. Mater. Res.* (2002) **32**, 113
39. Zhao, T., *et al.*, *Nat. Mater.* (2006) **5**, 823
40. Thole, B. T., *et al.*, *Phys. Rev. Lett.* (1985) **55**, 2086
41. Czekaj, S., *et al.*, *Phys. Rev. B* (2006) **73**, 020401(R)
42. Scholl, A., *et al.*, *Science* (2000) **287**, 1014
43. Scholl, A., *et al.*, *Rev. Sci. Instrum.* (2002) **73**, 1362
44. Nogues, J., and Schuller, I. K., *J. Magn. Magn. Mater.* (1999) **192**, 203
45. Bea, H., *et al.*, *Appl. Phys. Lett.* (2006) **88**, 062502
46. Lee, Y. H., *et al.*, *Electrochem. Solid-State Lett.* (2005) **8**, F55
47. Ueno, R., *et al.*, *Jpn. J. Appl. Phys.* (2005) **44**, L1231
48. Singh, S. K., *et al.*, *Appl. Phys. Lett.* (2006) **88**, 162904
49. Bea, H., *et al.*, *Jpn. J. Appl. Phys.* (2006) **45**, L187
50. Saito, K., *et al.*, *Jpn. J. Appl. Phys.* (2006) **45**, 7311
51. Chu, Y. H., *et al.*, *Appl. Phys. Lett.* (2007) **90**, 252906
52. Xu, G., *et al.*, *Appl. Phys. Lett.* (2005) **86**, 182905
53. Xu, G., *et al.*, *Appl. Phys. Lett.* (2006) **89**, 222901
54. Chu, Y. H., *et al.*, *Adv. Mater.* (2007), in press
55. Bea, H., *et al.*, *Phil. Mag. Lett.* (2007) **87**, 165
56. Holcomb, M. B., *et al.*, unpublished results
57. Chu, Y. H., *et al.*, *Adv. Mater.* (2006) **18**, 2307
58. Cruz, M. P., *et al.*, unpublished results
59. Shafer, P., *et al.*, *Appl. Phys. Lett.* (2007) **90**, 202909
60. Bea, H., *et al.*, *Appl. Phys. Lett.* (2005) **89**, 242114
61. Dho, J. H., *et al.*, *Adv. Mater.* (2006) **18**, 1445
62. Nolting, F., *et al.*, *Nature* (2000) **405**, 767